

## APPENDIX B

### Dual-wavelengths External-cavity Diode Lasers

The LCPM based dual-wavelengths ECDL system is discussed. The results of two wavelengths generation and their characteristics are demonstrated. Dual-wavelengths generated by using different LD sources, single stripe and broad area, are compared. The stabilities are also discussed. Finally, we present two possible methods for generating stable dual-wavelengths output.

#### B-1 Dual-wavelengths generation

A schematic of LCPM based ECDL is shown as Fig. 4.15. The LCPM is based on the design of a normally off-state TNLC cell bonded to a polarizer and an Au-coated silicon substrate as the back mirror. The TNLC cell is constructed with a 6- $\mu\text{m}$ -thick NLC (E7 manufactured by Merck) layer sandwiched between indium-tin-oxide (ITO) glass plates. One of the ITO electrodes is patterned. The pattern consists of fifty  $100\ \mu\text{m} \times 2\ \text{cm}$  stripes with 5- $\mu\text{m}$  spacing. The output from the AR-coated front facet of a LD is collimated by an objective lens (NA=0.55) and directed onto a grazing-incidence diffraction grating. Spectrally selective optical feedback is provided by the retro-reflected first-order-diffracted light from the grating, which is collected by an imaging lens and focused on the LCPM. The zeroth-order reflection beam from the grating is the useful output. In our experiment, the LD is usually operated at current  $I=1.4 I_{\text{th}}$ , where  $I_{\text{th}}$  is the threshold current. The gratings used for  $\lambda=800\ \text{nm}$  and  $\lambda=1.5\ \mu\text{m}$  are 1800 lines/mm and 1100 lines/mm, respectively. The laser wavelength is digitally tuned and switched by biasing the individual pixels of the LCPM, with wavelength steps  $d\lambda$  determined by the center-to-center separation of the adjacent pixel  $dx$  as Eq. (3.31).

$$d\lambda = \frac{a \cos \theta_m}{f_{\text{lens}}} dx \quad (\text{B.1})$$

A laser beam incidents on an 1800 lines/mm diffraction grating at an angle of  $85^\circ$ . The laser wavelength is 830 nm (SDL-2360). The focal length of the imaging lens is 250 mm. According to Eq. (3.31),  $d\lambda/dx = 1.833\ \text{nm/mm}$ . Thus the minimum and maximum spacing of

pixels are 0.193 nm and 9.4 nm respectively. It means that the wavelength spacing between the two wavelengths can be tuned from 0.193 nm to 9.4 nm in principle.

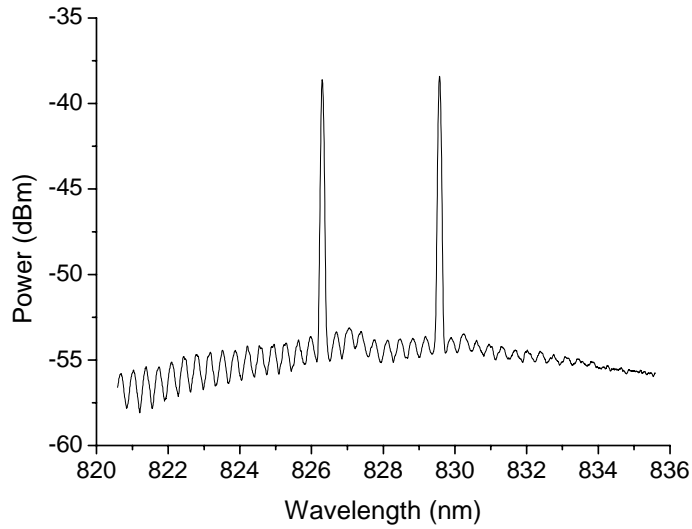


Fig. B.1 Typical dual-wavelengths lasing spectrum

By biasing two pixels at the same time, we obtain a co-axial dual-wavelengths output. Typical dual-wavelengths lasing spectrum is shown in Fig. B.1. Wavelength separation is 3.27 nm. The side-mode suppression ratio (SMSR) of each wavelength is better than 15 dB. The results of dual-wavelengths at different wavelength separations are demonstrated in Fig. B.2. Wavelength separations are 1 nm, 3.57 nm and 9.52 nm. The output power including two wavelengths is ~9 mW.

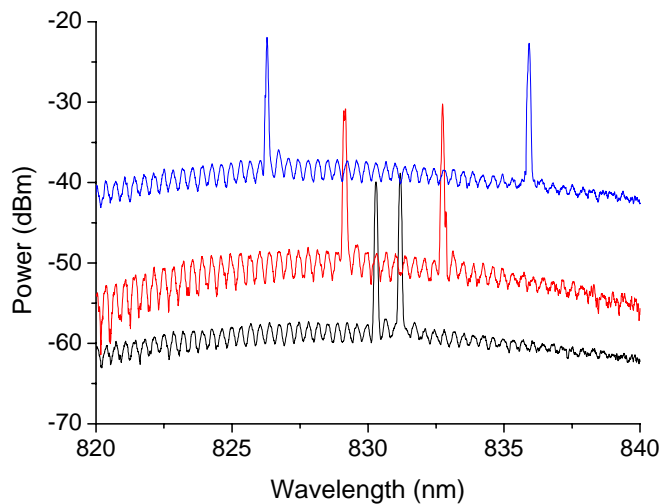


Fig. B.2 Dual-wavelengths spectra with wavelength separations of 1 nm, 3.57 nm and 9.52 nm

The two wavelengths output are collinear and have the same polarizations. We use a grating to separate the two wavelengths and to measure the output power of each wavelength by a power meter. In the experiment, we use an AR-coated LD with gain center at 1540 nm (Optospeed RSOA1550) and a grating with 1100 lines/mm. The SMSR of dual-wavelengths are better than 25 dB. The L-I curves of dual-wavelengths output are shown in Fig. B.3. As shown in the figure, the two wavelengths are not lasing simultaneously. One wavelength first achieves the threshold current ( $I=58$  mA) then the other ( $I=91$  mA). The power of first lasing wavelength achieves its maximum at a current of  $I=100$  mA, then it decreases when we keep increase the current. While the output power of the other wavelength increases. The two wavelengths achieve equal power at a current of  $I=103$  mA. Finally the wavelength with higher lasing threshold will dominate.

According to our present design, the diffraction efficiency of our grating is  $\sim 60\%$ . For a cw output of  $\sim 10$  mW, the laser power diffracted by the grating and focused onto the LCPM is  $\sim 6$  mW. The numerical aperture of the imaging lens is 0.2. Thus the spot size is  $\sim 10$   $\mu\text{m}$  in x direction and is  $\sim 40$   $\mu\text{m}$  in y direction due to dispersion effect. The power is focused and distributed in the area of  $5.25$  mm $\times 10$   $\mu\text{m}$  for the wavelength range of 13.2 nm. The intensity on the LCPM is thus  $11.4$  W/cm $^2$ .

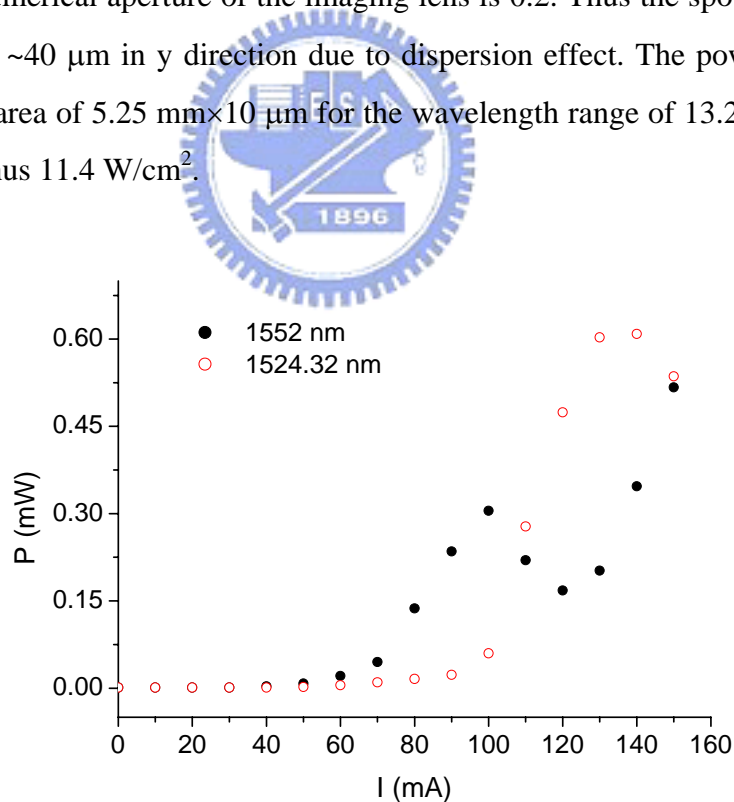


Fig. B.3 L-I curve of dual-wavelengths (1550 nm LD)

## B-2 Stability of dual-wavelengths

### 1. Dual-wavelengths spectrum

During the experiment, we can see the two wavelengths oscillate simultaneously when monitored by an OSA. Actually gain competition is drastic when we observed the spectrum by using a SFP simultaneously. As shown in Fig. B.4 (a)-(f), we demonstrate the spectrum of dual-wavelengths monitored by a SFP. The spectra are recorded at randomly time interval. The power difference between the two wavelengths is within 1 dB (measured by OSA) during the observing period. In Fig. B.4 (e) and B.4 (f), the two wavelengths oscillate at single longitudinal modes for only a short period of time. We change the power different between the two wavelengths by adjusting the applied voltages of the LCPM pixels individually. The power difference between the two wavelengths is varied from 2 dB to 9.3 dB. From Fig. B.5 (a) to (d), the spectra are arbitrarily taken by “freezing” the frame of the oscilloscope. Gain competition is obvious even the power of one wavelength is decreased to a half of the other ( $\Delta P=3$  dB). In Fig. B.5 (e) and B.5 (f), the power difference is large and only the one with higher gain oscillates. At the same time we still can see the dual-wavelengths spectrum on the OSA. Though we can generate two wavelengths and they seem to be exist simultaneously, actually they are not stable enough. The dual-wavelengths can not exist as long as we wish.

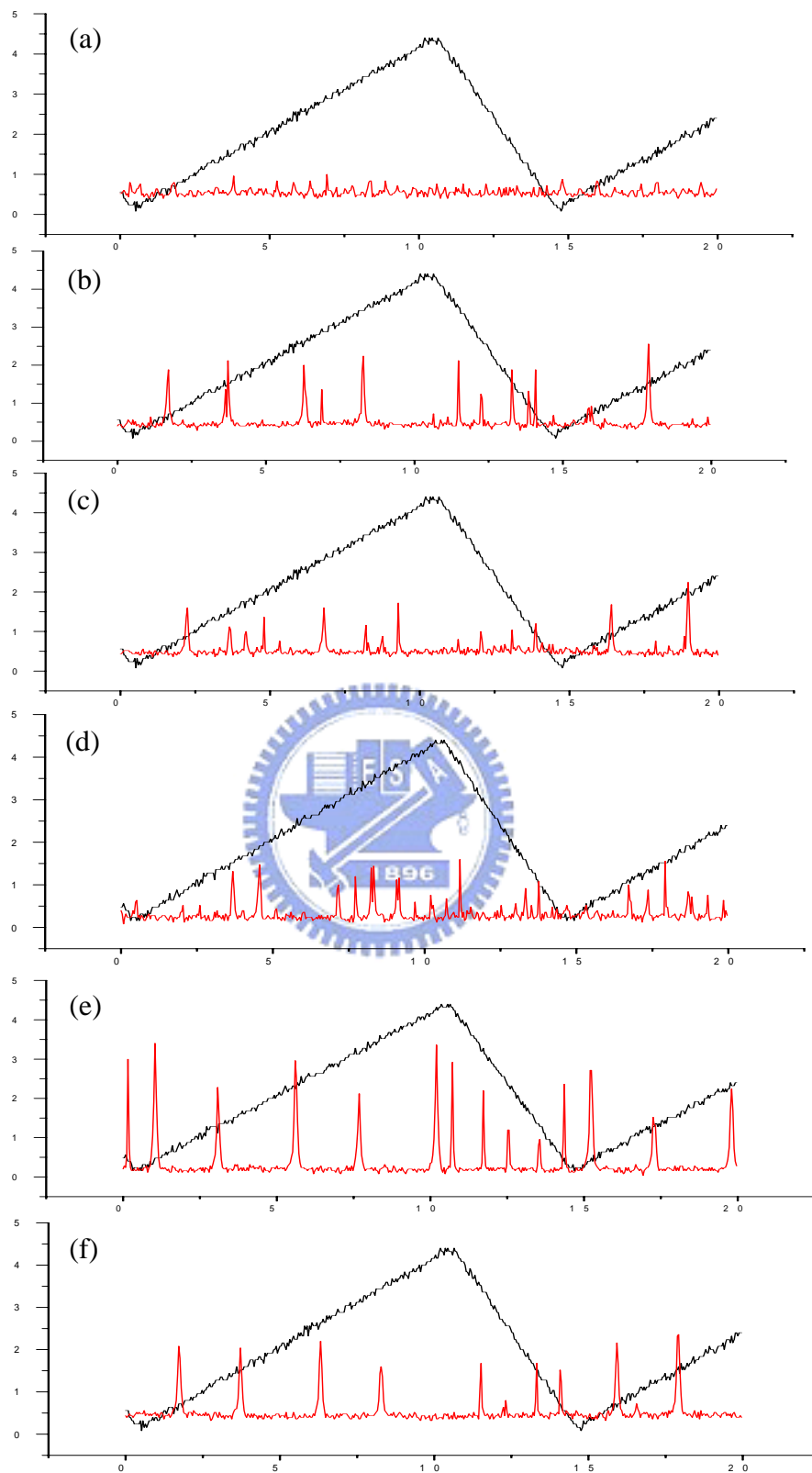


Fig. B.4 Dual-wavelengths spectrum monitored by a SFP at randomly time intervals

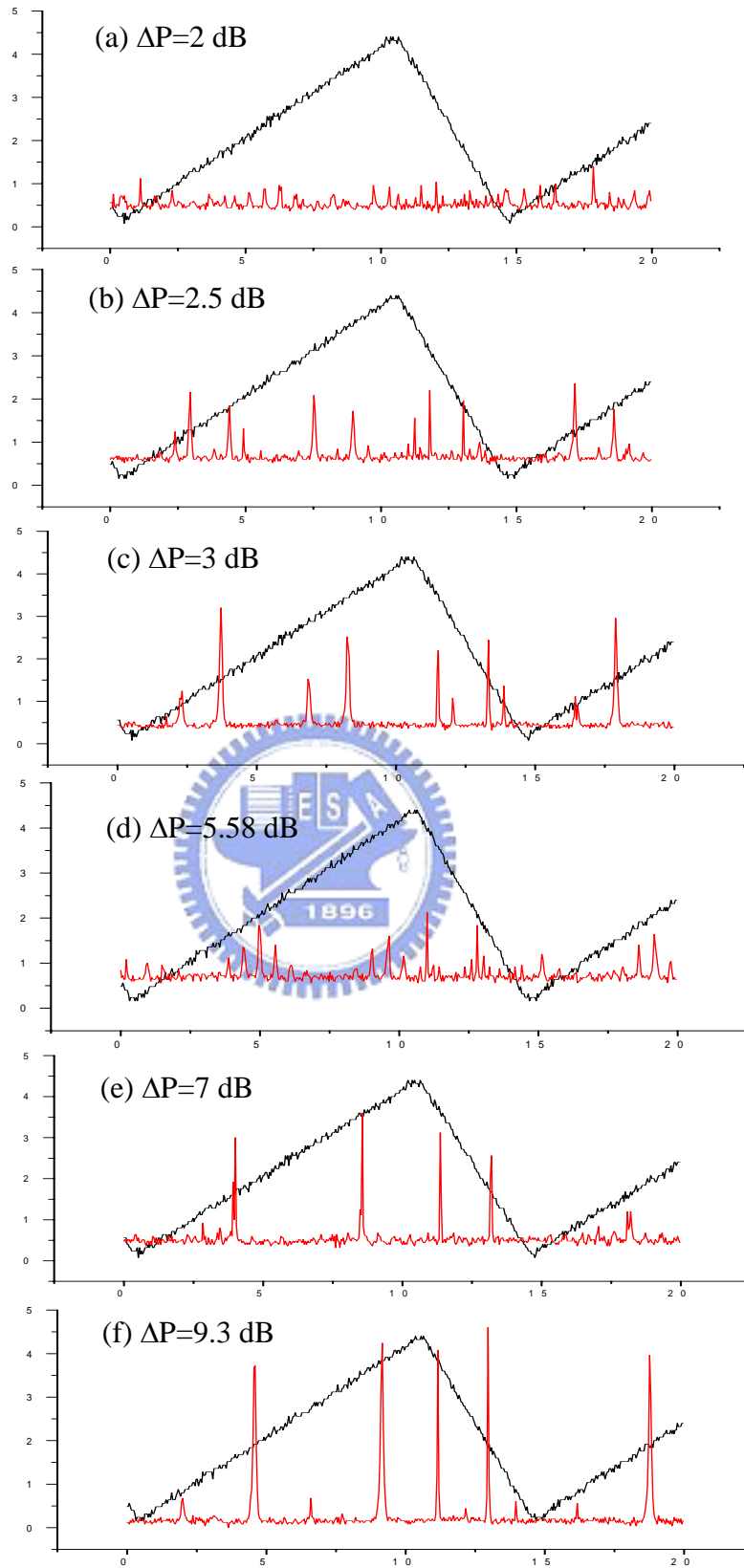


Fig. B.5 Dual-wavelengths spectrum with power differences form 2 dB to 9.3 dB

## 2. Single strip versus broad area LD's

In the experiment of dual-wavelengths generation, we use two different LD sources. A LD, which gain center is at 772 nm is a single stripe LD (SS-LD, SAL-780). And another with gain center at 830 nm is a broad area LD (BA-LD, SDL-2360). The power fluctuations of dual-wavelengths generated by using each LD are observed and demonstrated in Fig. B.6.

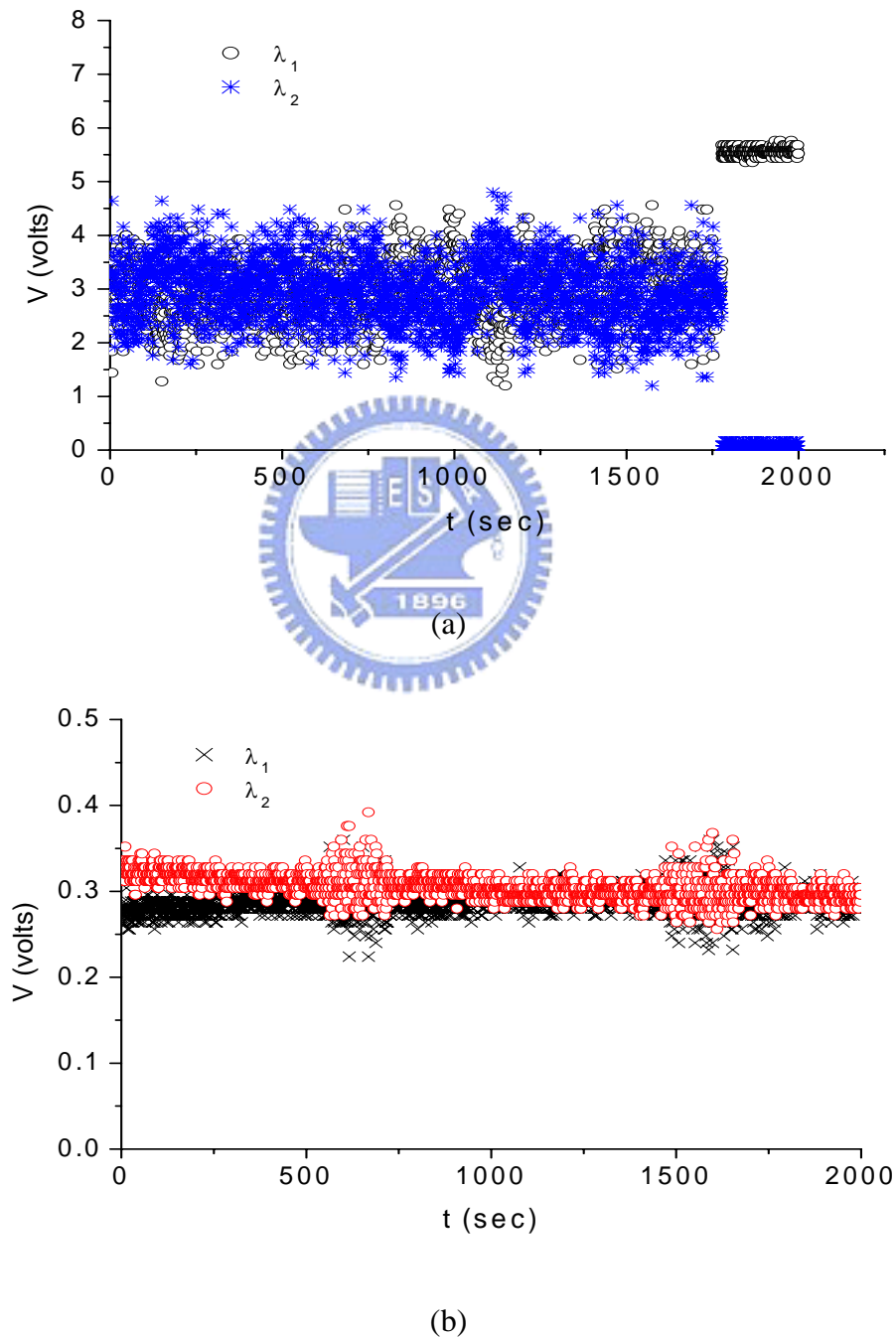


Fig. B.6 Dual-wavelengths power fluctuations of (a) single stripe LD and (b) broad area LD

The two wavelengths output are collinear. We use a grating to separate the two wavelengths. The output intensity of each wavelength is measured by a photodiode. The output powers of the two wavelengths are adjusted to be as equal as possible. The power fluctuations are observed simultaneously for a period of about 30 minutes. The power fluctuation of two wavelengths generated by using the SS-LD is shown in Fig. B.6 (a). It is obvious that the power fluctuations are violent when two wavelengths oscillate simultaneously. If we switch one wavelength ( $\lambda_2$ ) off and let only one wavelength ( $\lambda_1$ ) oscillates, the power fluctuation is smaller. It is about one fifth of the range of power fluctuations compared with that of two wavelengths oscillate. One wavelength competed with the other in gain. In Fig. B.6 (b), we demonstrate the power fluctuation of the BA-LD. The gain competition is not as severe as for the SS-LD. The power fluctuation  $\Delta p/p$  is less than a half of that compared with using the SS-LD. We can conclude that dual-wavelengths generated by using the BA-LD is stable than generated by using the SS-LD

### B-3 Stable dual-wavelengths generation

We have concluded that the power fluctuations of dual-wavelengths are smaller by using the BA-LD. It doesn't mean that we can achieve stable dual-wavelengths output by using a BA-LD as the light source. If we observe the optical spectrum by a SFP, the spectra are the same as we have shown in Fig. B.4 and B.5. The spectra are derived by using the SS-LD and BA-LD respectively. They are not stable enough no matter what kind of light sources are used. Stable dual-wavelengths output is important for cw terahertz generations. We would like to have stable dual-wavelengths generation and it can exist long enough for terahertz detections.

In next two sections, we present two possible methods for generating stable dual-wavelengths output. One method is to employ a special designed étalon in the laser cavity. The other method is mutual injection of an ECDL and a semiconductor optical amplifier (SOA).

#### B-3.1 LCPM based ECDL with an intracavity étalon

The concept of employing an étalon in the laser cavity is based on wavelength filtering. The étalon is designed that its FSR is equal to the wavelength spacing of the LCPM pixels. Only the wavelength selected by the pixel matched the wavelength selected by the étalon can oscillate. The schematic of the LCPM based ECDL with an intracavity étalon is shown as Fig.

B.7.

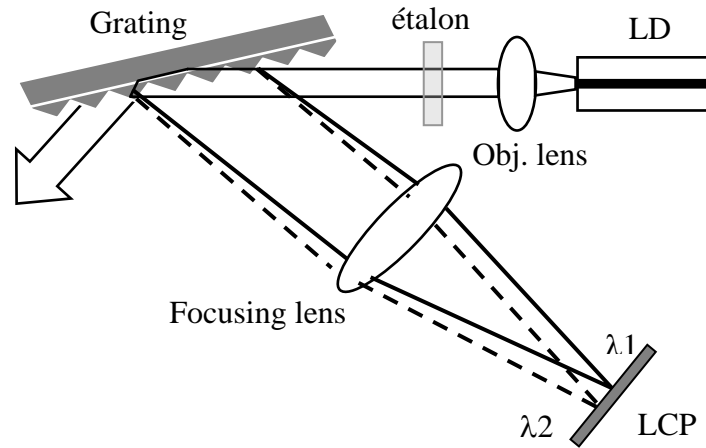


Fig. B.7 LCPM based ECDL with an intracavity étalon

We design the étalon based on the system specifications of input wavelength  $\lambda=830$  nm, grating pitch=1800 lines/mm, angle of incidence  $\theta_i=75^\circ$ , focal length=15 cm, pixel pitch=105  $\mu\text{m}$ . According to Eq. (3.31), the wavelength spacing between adjacent pixels is 0.33 nm or 143.7 GHz. The manufacturing specifications of the étalon are listed in Table B.1. The FSR of the étalon is calculated to be  $\sim 142.9$  GHz. The resolution is 7.1 GHz.

Table B.1 Specifications of the designed étalon

material	diameter	thickness	finesse	flatness & parallelism
Fused silica	12.7 mm	$0.7\pm 0.05$ mm	20	$\lambda/10$

In the experiment, we use a 780 nm SS-LD as a light source. The spectra of before and after employing an intracavity étalon are shown in Fig. B.8. In the figure, the upper profile is the single wavelength lasing spectrum of the ECDL without the étalon. The lower profile is the étalon spectrum when system does not lasing. The étalon mode (FSR) is measured to be 0.29 nm (or 145.6 GHz). We can see that it is different from the laser cavity mode. For a 60-cm cavity, the cavity mode is 0.25 GHz. The single wavelength lasing spectra of introducing the étalon are demonstrated in Fig. B.9 (a) and (b). Actually two pixels of the LCPM are in on-state during the experiment but we only let one wavelength lasing. The spectrum of Fig. B.9 (a) is observed by an OSA. The lasing wavelength is one of the selected étalon modes. The étalon modes can be clearly seen. Though the étalon modes seem to be

significant, it is a purely single longitudinal output when we observed the spectrum by a SFP (Fig. B.9 (b)).

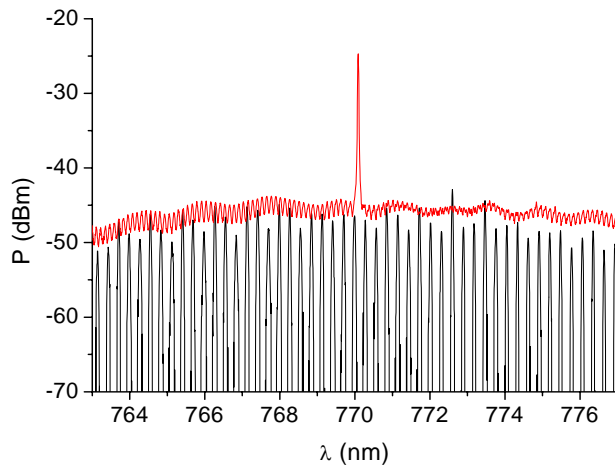
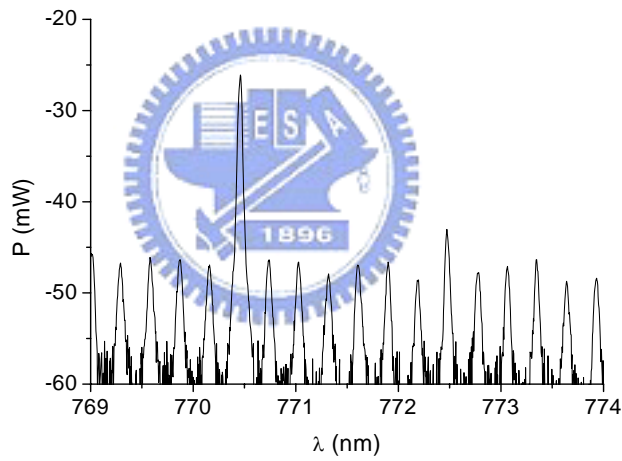
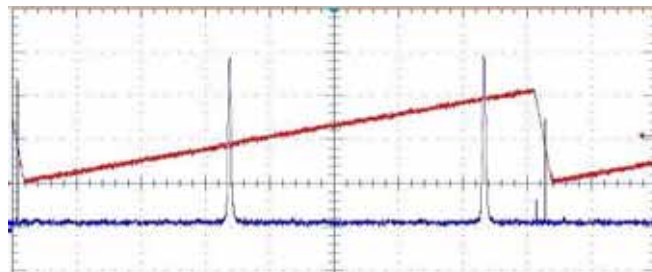


Fig. B.8 Optical spectra without and with employing an étalon



(a)



(b)

Fig. B.9 Single wavelength spectrum observed by an OSA (a) and a SFP (b) when employ an intracavity étalon

The dual-wavelengths spectrum of the LCPM based ECDL with an intracavity étalon is shown in Fig. B.10. Wavelength spacing is 2.02 nm. The spacing of the étalon modes is 0.29 nm. Fig. B.11 (a) and (b) demonstrates the spectrum monitored by a SFP. As we have mentioned in Sec. B-1, the two wavelengths are not lasing simultaneously. One wavelength ( $\lambda_1$ ) first achieves the threshold current then the other ( $\lambda_2$ ). In Fig. B.11 (a), we demonstrate the dual-wavelengths spectrum when  $\lambda_2$  just achieves its threshold current. At this status, the power of  $\lambda_1$  is larger than  $\lambda_2$ . Side modes (small peaks) are not suppressed completely though they are small. When the power of the two wavelengths are nearly equal, side modes are enhanced and main peaks of the two wavelengths become uneasy to be recognized (Fig. B.11 (b)). The spacing of the adjacent side modes is  $\sim 0.25$  GHz, which is equal to the cavity mode spacing.

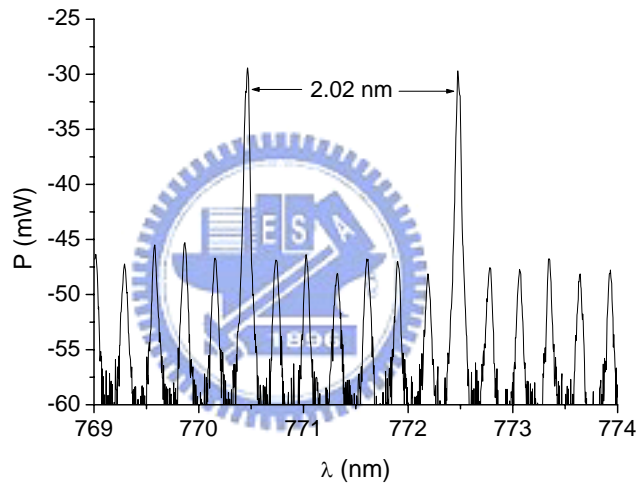
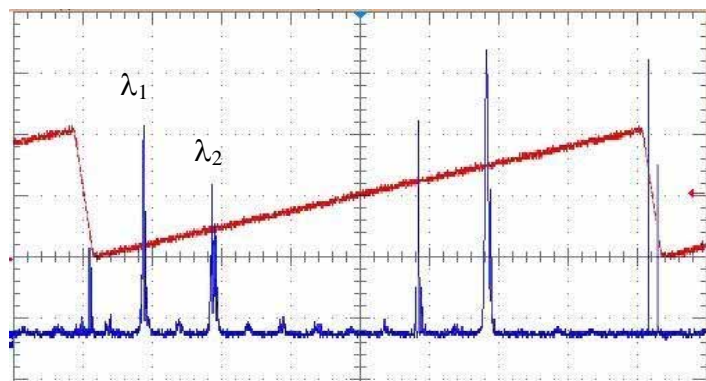
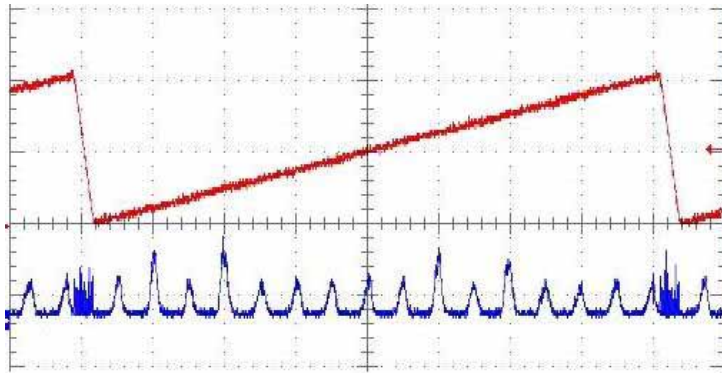


Fig. B.10 Dual-wavelengths étalon-employed spectrum.



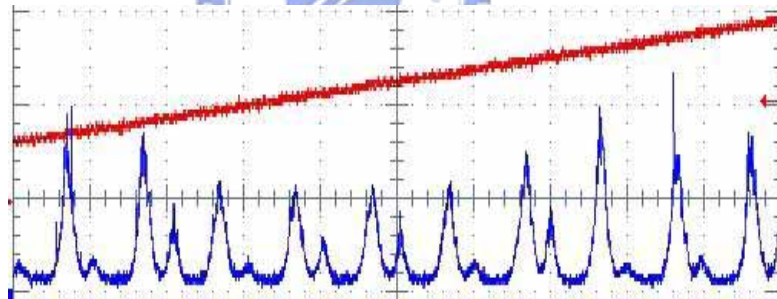
(a)



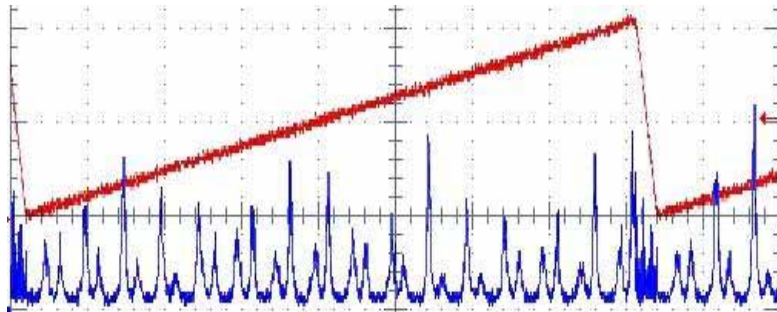
(b)

Fig. B.11 Dual-wavelengths spectra at the status of (a)  $\lambda_2$  is just lasing; (b) the power of  $\lambda_1$  and  $\lambda_2$  are nearly equal

In above situations, the gain competition is still violent. The dual-wavelengths output is not in stable state. The stable state can be achieved at the status as shown in Fig. B.12 (a) or (b). If we separate the two wavelengths by a grating, we can find two bright spots on a screen. The two spots remain stable and the gain competition is not significant. As can be seen from the figure, both the wavelengths are not single longitudinal modes output.



(a)



(b)

Fig. B.12 The spectra of stable dual-wavelengths with (a) unequal and (b) nearly equal power

### B-3.2 Mutual injection of an ECDL and a SOA

In this section, we describe the method of mutual injection of the LCPM based ECDL and a SOA. The purpose of mutual injection is to flatten the gain profile of the LD. Typically the gain profile of the LD is not flat. If we enhance the area of lower gain by injecting a higher gain, the gain profile could be much flat. Thus the gain competition in this area may alleviate. Furthermore, the feedback from the SOA and the cavity loss of the ECDL compensate for each other, which helps in suppressing the side modes. Then we can expect stable dual-wavelengths output. The experimental setup for mutual injection is shown in Fig. B.13. An ECDL and a SOA are feedback injected into each other. The dotted frame area is the LCPM based ECDL. Though the LD (SAL-830-SN1) we use in the ECDL is AR-coated, self-lasing happens at the current of 45 mA at 20 °C. The gain bandwidth of the LD is 20 nm. The SOA (SDL-2360) is an AR-coated BA-LD. The threshold current at 20 °C is 398 mA. The output power is ~60 mW at operating current of 600 mA. Because the output of SOA has serious astigmatism, we use an anamorphic prism pair for correcting the beam shape in order to achieve better injecting efficiency. The difference between gain centers of the LD and SOA at 20 °C is 12 nm. The gain profiles are plotted in Fig. B.14. We can make gain centers of both closer by changing the operating temperatures. When the LD and the SOA are operated at 28 °C and 11 °C, gain centers are 822.5 nm and 819 nm respectively, the difference in gain centers is 3.5 nm.

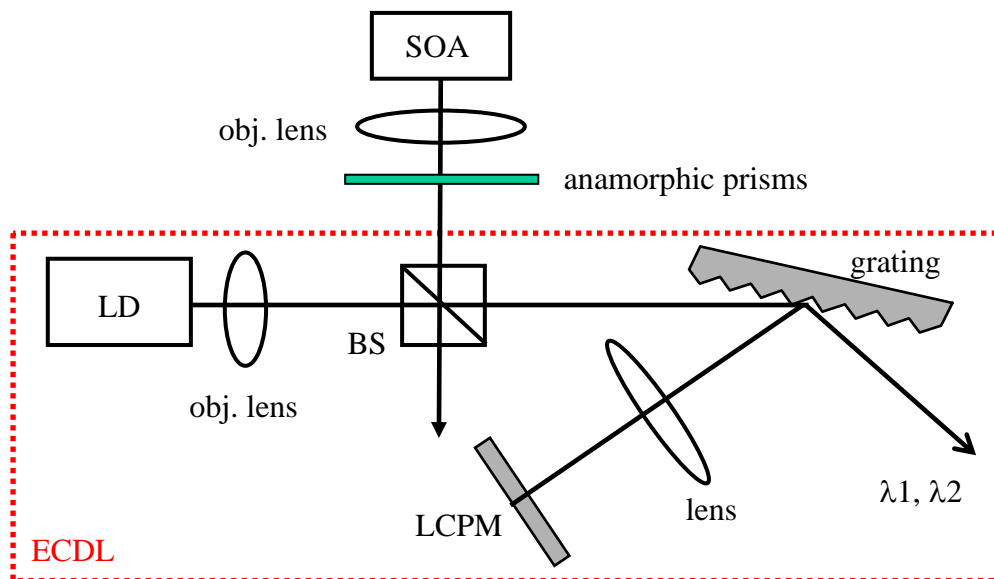


Fig. B.13 Experimental setup of mutual injection

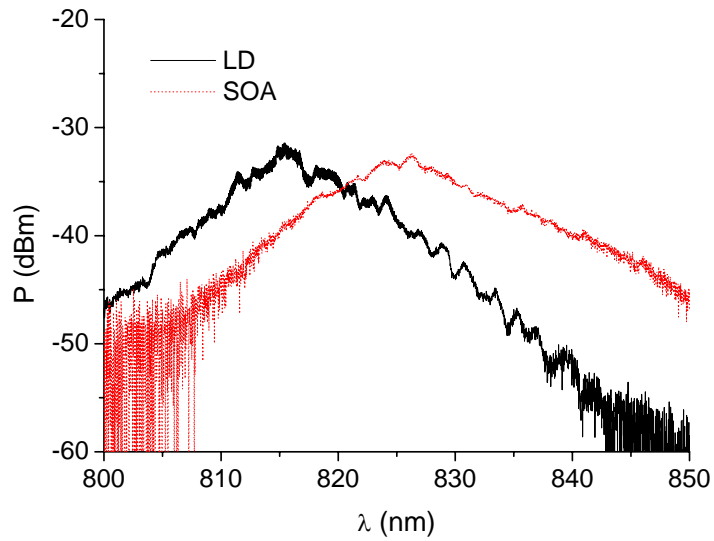


Fig. B.14 Gain profiles of the LD and SOA at 20 °C

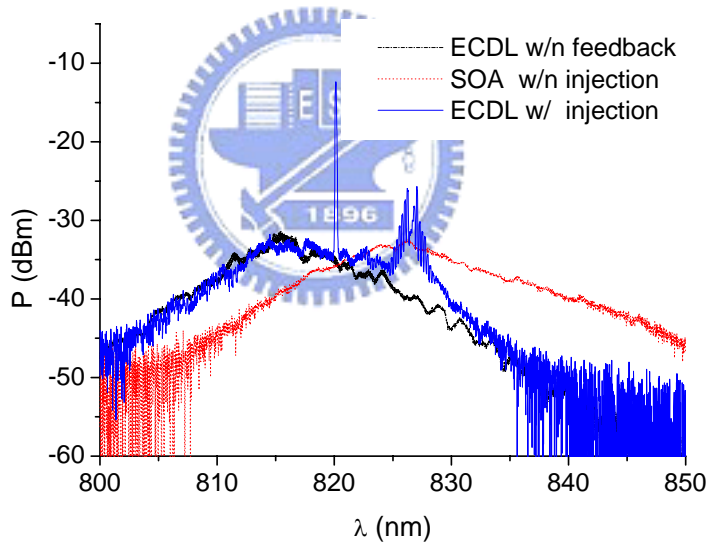


Fig. B.15 Lower gain area of the LD is enhanced by injection of the SOA

The lower gain area of the LD enhanced by injection of the SOA is shown in Fig. B.15. Gain profiles of the LD and the SOA are demonstrated by the dotted-dash line and the dotted line. The solid line is the single wavelength lasing spectrum of the ECDL when injection. The region of the gain profile of the LD, which near the gain center of the SOA is enhanced by injection. The results of single wavelength mutual injections are demonstrated in Fig. B.16. The LD and the SOA are operated at 25 °C and 11.5 °C, the difference in gain centers is 7 nm. The lasing wavelength (822.5 nm) is closer to the gain center of the SOA (824.5 nm) than to

the gain center of the LD (817.5 nm). We observed the spectra of the ECDL and the OSA simultaneously. The SMSR is 25.5 dB and 11 dB of the ECDL and the SOA respectively.

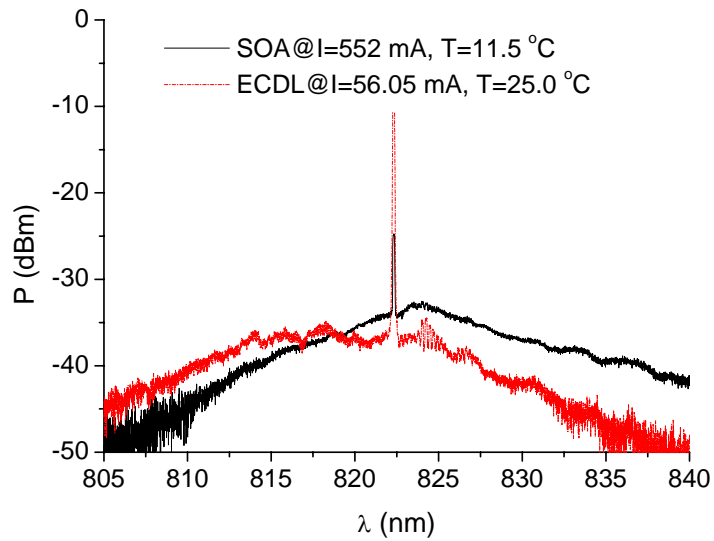
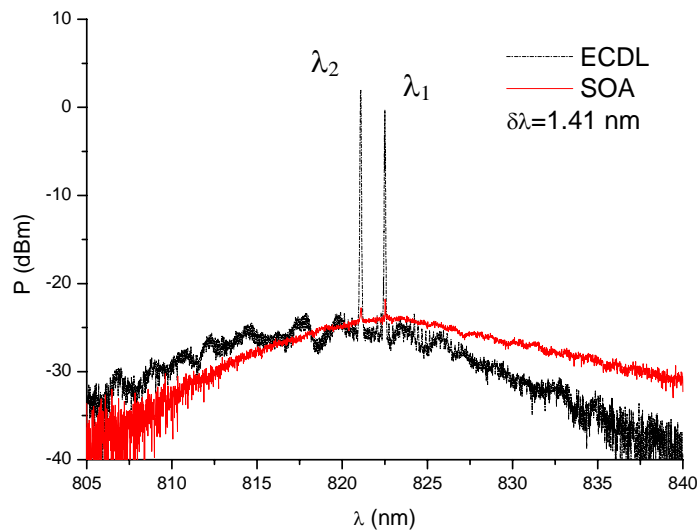
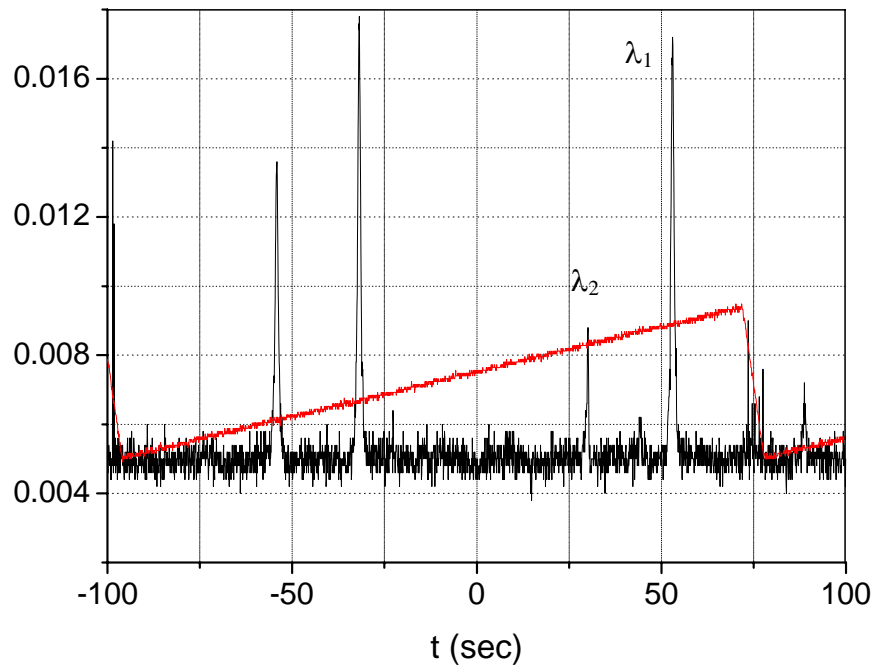


Fig. B.16 Single wavelength lasing spectrum of the ECDL and SOA when mutual injection

The results of dual-wavelengths mutual injection are demonstrated in Fig. B.17 (a)(b) and Fig. B.18 (a)(b). The LD and the SOA are operated at 30 °C and 11 °C. The difference between gain centers is 3.5 nm. In Fig. B.17 (a) and B.18 (a) are the lasing spectra observed by an OSA. In Fig. B.17 (b) and B.18 (b) are the spectra observed by a SFP. The spacing of the two wavelengths ( $\delta\lambda$ ) is 1.41 nm and 5.4 nm in Fig. B.17 and Fig. B.18, respectively.

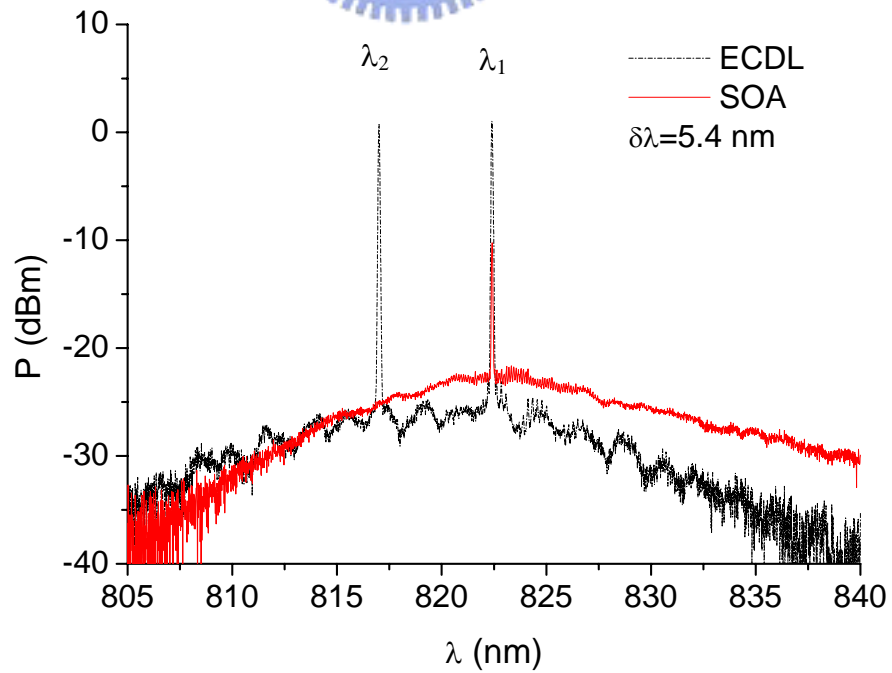


(a)



(b)

Fig. B.17 Dual-wavelengths generation when mutual injection ( $\delta\lambda=1.41$  nm).  
The spectrum are observed by (a) SOA and (b) SFP



(a)

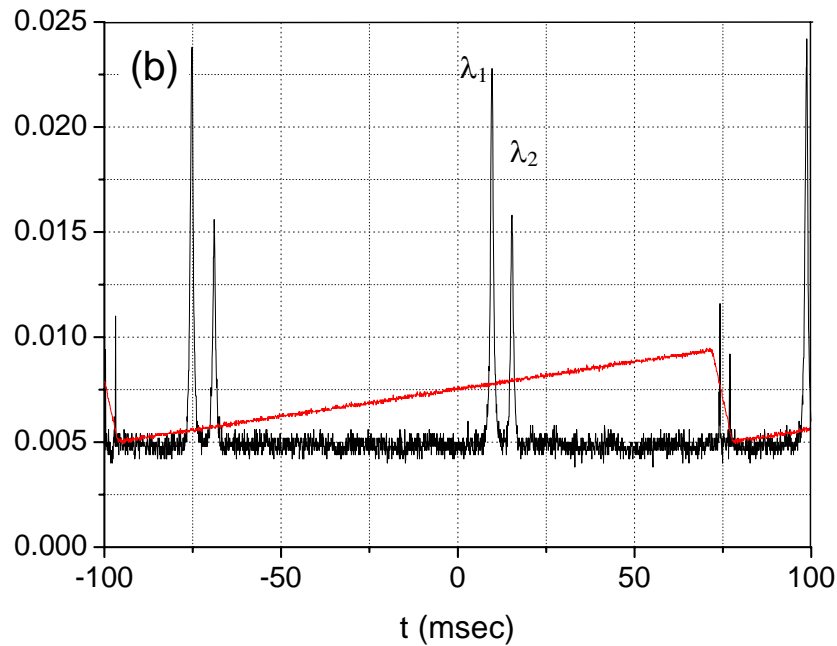


Fig. B.18 Dual-wavelengths generation when mutual injection ( $\delta\lambda=5.4$  nm).

The spectrum are observed by (a) SOA and (b) SFP

In Fig. B.17, both wavelengths  $\lambda_1$  and  $\lambda_2$  are near the gain center of the SOA. Two peaks though small can be seen on the spectrum of SOA. The small signal is due to the large beam size of the SOA. The injection power is approximately one fifth of the total output power of the SOA. In Fig. 5.22, the two wavelengths are adjusted to be symmetrical to the gain center of the LD. The wavelength  $\lambda_1$  is near the gain center of the SOA. When we observe the spectrum by the SFP as shown in Fig. B.17 (b) and B.18 (b), the two wavelengths can be easily recognized and both are in single longitudinal modes. Mutual injection induces the noise suppression effect, but the stability of the dual-wavelengths does not appear improved. Gain competition is still severe.